JOURNAL OF APPLIED ELECTROCHEMISTRY 21 (1991) 84–90

Electrochemical behaviour of tin in bicarbonate solution at pH 8

M. DROGOWSKA, H. MÉNARD

Département de Chimie, Université de Sherbrooke, Sherbrooke, Québec J1K 2R1, Canada

L. BROSSARD

Institut de Recherche d'Hydro-Québec (IREQ), PO Box 1000, Varennes, Québec J0L 2P0, Canada

Received 25 October 1989; revised 15 May 1990

The anodic oxidation of tin in 0.1 to 1 M bicarbonate solutions at pH 8 has been studied. The process may be divided into three potential regions: (1) a short active dissolution (Tafel) region; (ii) a dissolution-precipitation region; and (iii) a large region of electrode passivity. The rate-determining step of the reaction in the active-dissolution region is attributed to the diffusion of an ionic species into the solution, the diffusing species being generated at the metal surface. In the region of the first oxidation peak, the reaction rate is controlled by diffusion of CO_3^{2-} species in solution. When the potential becomes more positive than $-0.1\ V_{sce}$, a highly passivating (most likely SnO_2) film is formed on the electrode surface.

1. Introduction

Much of the literature on the electrochemistry of tin is devoted to its behaviour in alkaline solutions at pH > 12 [1–10]; comparatively little attention has been given to its behaviour in a neutral media [11, 12]. Examination of the potential against pH equilibrium diagrams in [13–15] indicates that a tin electrode can be active or passive, depending on the applied potential. Since the solubility of the various tin oxides goes through a minimum at a pH close to 8.5, owing to the amphoteric nature of the metal, the resistance of tin to corrosive attack by most neutral solutions is good because of the presence of oxide films. There is some disagreement regarding the composition of the film, however, and the electrochemical oxidation mechanism remains unclear.

Thermodynamic considerations suggest many possible oxidation reactions for tin in aqueous solutions [1, 2, 13–18]. The occurrence of mixed-state oxides and hydroxides of tin may be expected, as the standard potentials for Sn/SnO and Sn/SnO_2 systems are close, namely $-0.818\ V_{sce}$ and $-0.820\ V_{sce}$ at pH 8 respectively, while the difference between the potentials of Sn/SnO and $Sn(OH)_2$ is only 12 mV. Dissolved tin species may therefore be precipitated from the solution as an oxide or hydroxide; however, hydroxides are unstable with respect to the corresponding oxides and highly irreversible dehydration is favoured. Hydration of the oxides is therefore thermodynamically improbable.

$$SnO(s) + H_2O = Sn(OH)_2(s)$$
$$\Delta G = 2.5\ kJ\ mol^{-1}$$
$$SnO_2(s) + 2H_2O = Sn(OH)_4(s)$$
$$\Delta G = 37.3\ kJ\ mol^{-1}$$

Nevertheless, the dehydration of $Sn(OH)_2$ is complete only at high temperatures, at $T \sim 100°C$ [13, 14]. This compound can undergo both progressive dehydration [15] to $2SnO \cdot H_2O$, $5SnO \cdot 2H_2O$, $3SnO \cdot H_2O$ and SnO, and oxidation to $SnO_2 \cdot nH_2O$ is also irreversible. The rate of these reactions is known to be slow, although it may be increased by applied electric field. On the other hand, stannic hydroxides may exist as gels, which do not correspond to the stoichiometric formula $Sn(OH)_4$ and crystallize progressively to cassiterite, SnO_2 [13]. However, various solid phases may form and the mixture of stannous and stannic oxides may coexist although, at equilibrium, SnO_2 is the predominant passivating species. The solubility data of tin oxides and hydroxides are limited and are accurate only for very acidic or alkaline solutions but generally, the solubility of Sn(II), calculated from ΔG values, is greater than that of Sn(IV) [15].

In practice, tin is used as an electrodeposited coating on steel, copper and nickel to protect them against corrosion and is therefore exposed to attack by various solutions. For example, underground metallic structures coated with tin may be in contact with aqueous carbonate solutions [19]. Although under certain conditions, carbonate-bicarbonate ions have a considerable influence on the corrosion and passivation of metals, only one publication [11] has dealt with the galvanostatic study of the behaviour of tin in 0.1 M $NaHCO_3$ solution. The present investigation was directed towards establishing the electro-dissolution and passivation processes of tin in carbonate solution. The experiments were carried out in solutions containing 0.1 to 1 M $NaHCO_3$ at pH 8 and 25° C.

2. Experimental details

The measurements were performed in a conventional

0021-891X/90 $03.00 + .12

two-compartment, three-electrode electrochemical cell using a tin rotating disc electrode or stationary disc electrode 0.13 cm^2 in surface area, cut from a polycrystalline tin rod (Johnson Matthey Chem. Ltd., grade 1) and set in a Kel-F holder. The electrode surface was polished with an alumina suspension and rinsed in distilled water. The auxiliary electrode was a platinum grid separated from the main compartment by a Nafion membrane. The reference electrode was a saturated calomel electrode (SCE) separated from the main compartment by a salt bridge with a Luggin capillary. All potentials quoted below are given with reference to this electrode.

Solutions of 0.1 to 1 M $NaHCO_3$ were prepared with Baker analysed grade reagent. No buffer or support electrolyte was used. Before each experiment the pH was measured and the solution was deoxygenated with nitrogen, which was maintained above the solution at all times. The measurements were carried out at 25° C.

The potential applied to the working electrode by a PAR 273 poteniostat was controlled by a pulse generator with a PAR 175 universal programmer. The current-time transients were recorded with a Commodore PCII microcomputer using a GPIB-PC-2A interface or, for microsecond records, with a Computerscope interface (R.C. Electronic Inc). Electrode rotation was performed using an Analytical Rotator Pine Instrument.

3. Results

The polycrystalline tin electrode was first immersed in the solution with the potentiostat at -1 V to remove any surface oxides and when the cathodic current was lower than 0.4 $\mu A\,cm^{-2}$, the electrode was considered satisfactory. The electrochemical behaviour of the electrode rotated at 1000 r.p.m. with a scan rate dE/dt of 10 $mV\,s^{-1}$ is illustrated by the polarization curves in Fig. 1, which represent tin undergoing passivation. Two oxidation peaks, A_1 and A_2, at -0.8 V and -0.65 V respectively, and a large passivation region, between -0.1 V and $+1.8$ V, were observed. As the concentration of $NaHCO_3$ solution increased, so did the height of the anodic peaks, while the passivation current remained independent of the concentration effect. On the cathodic side, only one peak, C_1, occurred at -1.1 V, and it was immediately apparent that the oxidation charge was much greater than the reduction charge. At the limits of the potential scan, at $+1.8$ V and -1.3 V, oxygen and hydrogen were evolved.

3.1. *Steady-state measurements*

The potentiostatic method was used for the steady-state measurements. The current against time curves for various values of the anodic applied potential were recorded by a computer until the steady-state current was obtained. The potential step started from the open-circuit potential and rose to the desired anodic potential.

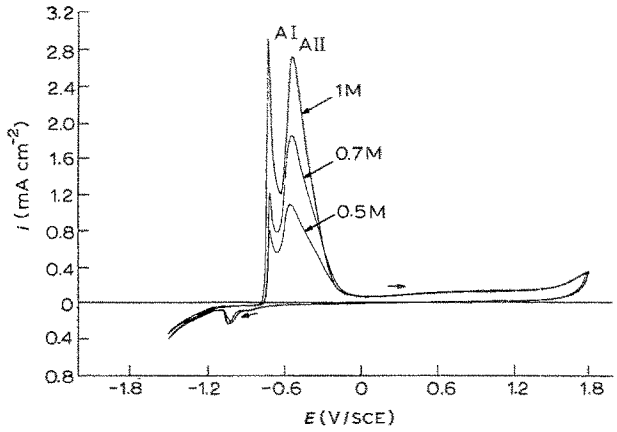

Fig. 1. Typical cyclic voltammogram for a tin disc electrode rotated at 1000 r.p.m. and $dE/dt = 10\,mV\,s^{-1}$ in $NaHCO_3$ solutions at pH 8.

In the current-time transient two different behaviours were displayed (Fig. 2). When the potential pulse was in the region of active dissolution, the current increased to a steady-state value (curve a) whereas rapidly falling current transients (curve b) were obtained in the semipassive and passive potential ranges. This decrease in the current-time transient is consistent with the case of random film deposition, for which the current decreases continuously to zero. No peak was observed in the current transients, indicating that a nucleation and growth process was not involved.

The steady-state current against potential curves were very similar to those in Fig. 1 obtained by a potential-sweep technique, the principal difference being that the current fell to zero in the second passivation region.

The results for the region of active dissolution presented as plots of log i against E for five concentrations of $NaHCO_3$ solutions between 0.1 and 1 M at pH 8 and 1000 r.p.m. are shown in Fig. 3. The log–linear relationship gives the slopes

$$\left\{\frac{dE}{d\log i}\right\}_{pH\,8} \sim 27\,mV\,dec^{-1} \qquad (1)$$

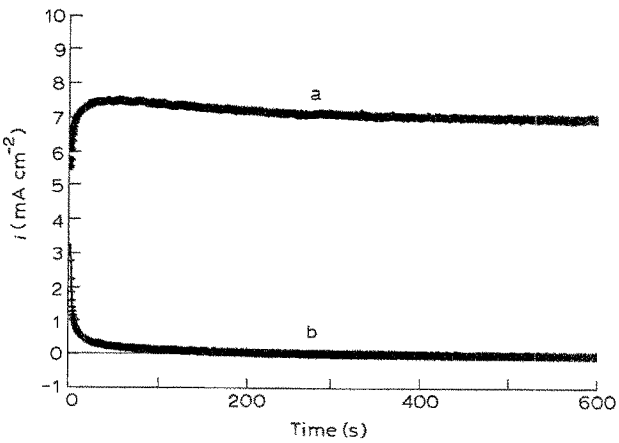

Fig. 2. Potentiostatic current-time transient for a tin disc electrode rotated at 10000 r.p.m. in 0.5 M $NaHCO_3$ solution at pH 8 and at two different potentials: (a) -0.81 V (Tafel region); (b) 0.69 V (passivation region).

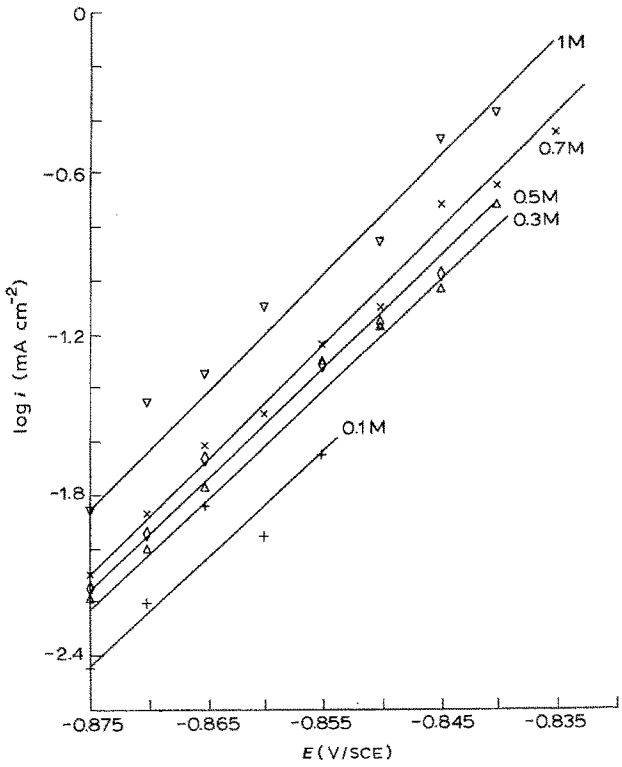

Fig. 3. Tafel plots, log i against E, for a tin disc electrode rotated at 1000 r.p.m. in 0.1 to 1 M $NaHCO_3$ solutions at pH 8.

The value of this slope was independent of the electrode rotation rate, but the current rose as the $NaHCO_3$ concentration and the electrode rotation speed were increased. The current is plotted as i_{ss} against $\omega^{1/2}$, for 0.5 M $NaHCO_3$ solution at constant applied potentials in Fig. 4; the relationship is a straight line passing near zero for $\omega^{1/2} \to 0$, in accordance with the Levich theory [20] for a diffusion-controlled process:

$$\left\{\frac{di}{d\omega^{1/2}}\right\}_{E,HCO_{3,pH8}^-} = \text{constant} \qquad (2)$$

The slope of $di/d\omega^{1/2}$ increased with the applied potential to give

$$\left\{\frac{dE}{d\log(di/d\omega^{1/2})}\right\}_{HCO_{3,pH8}^-} \sim 30\,\text{mV dec}^{-1} \qquad (3)$$

The order of reaction against the HCO_3^- ion concentration is equal to 1.5

$$\left\{\frac{d\log i_{ss}}{d\log[HCO_3^-]}\right\}_{-0.85\,V,pH8} = 1.5 \qquad (4)$$

but, as the ionic strength was not kept constant, only qualitative conclusions may be drawn from the measured value. By adding an appropriate quantity of salt to keep the ionic strength constant, the behaviour of the corrosion process may be completely changed.

3.2. *Cyclic voltammetry experiments*

The cyclic voltammetry experiments were used to investigate the influence of (i) potential scan limits, (ii) rotation speed and (iii) sweep potential rates on the anodic and cathodic currents and charges.

Figure 5 shows a series of voltammograms reversed at progressively increasing potentials for a tin disc electrode rotated at 1000 r.p.m., 10 mV s^{-1}, in 0.5 M $NaHCO_3$ solution at pH 8. For the curves with anodic potential limits up to −0.1 V, the corresponding negative-going potential sweep showed an anodic current. The lack of reduction current and the rising anodic current with two maxima indicated that the anodic dissolution reaction of tin still occurred, even in the negative scan direction.

When the upper potential limit exceeded −0.1 V, the anodic current reached a passivation plateau ($i \sim 10\,\mu A\,cm^{-2}$) and remained there until the evolution of oxygen. On the reverse potential sweep, the electrode retained its passivity with near-zero current, the anodic current on the negative-going potential

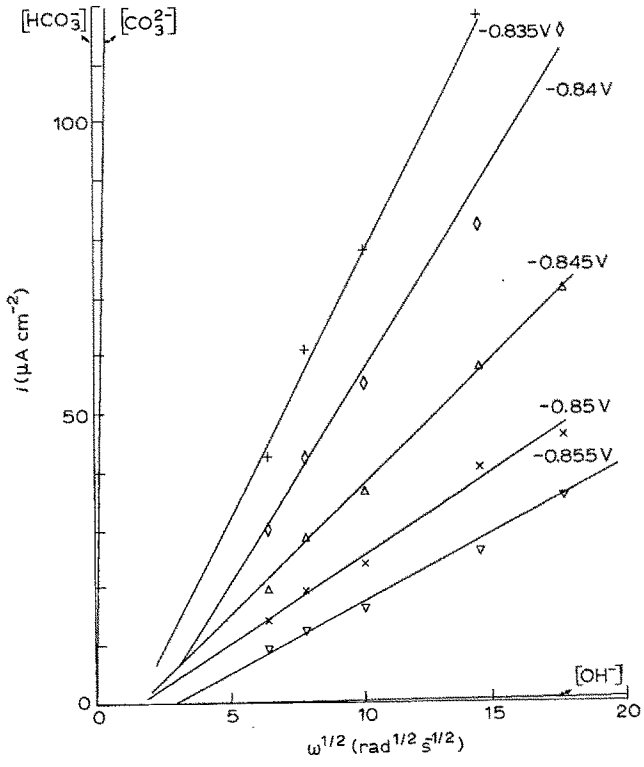

Fig. 4. Steady-state current against $\omega^{1/2}$ plot for different potentials in the Tafel region, 0.5 M $NaHCO_3$ solution at pH 8, for a tin disc. Theoretical curves calculated from Equation 6 from diffusion of OH^-, HCO_3^- and CO_3^{2-} species.

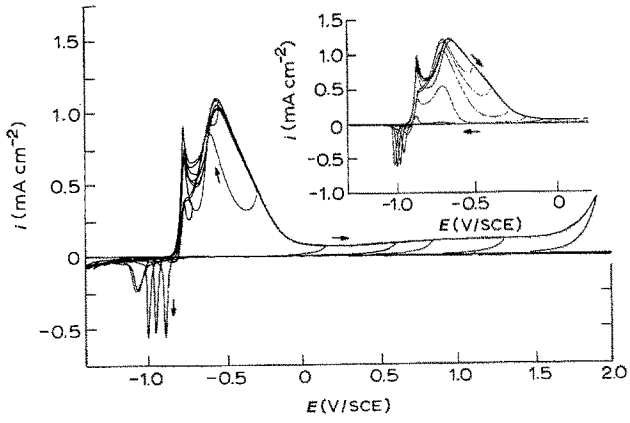

Fig. 5. Cyclic voltammograms reversed at progressively increasing positive-potential limits for a tin disc electrode rotated at 1000 r.p.m. in 0.5 M $NaHCO_3$ solution, at pH 8 and dE/dt = 10 mV s^{-1}.

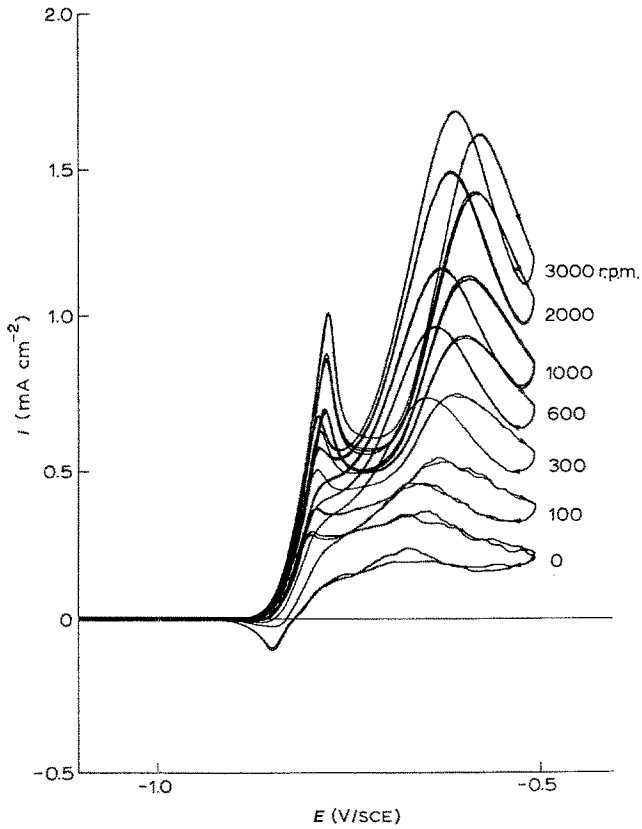

Fig. 6. Cyclic voltammograms for a tin disc electrode rotated at various speeds from 0 to 3000 r.p.m. at $dE/dt = 10\,mV\,s^{-1}$ in 0.5 M $NaHCO_3$ at pH 8.

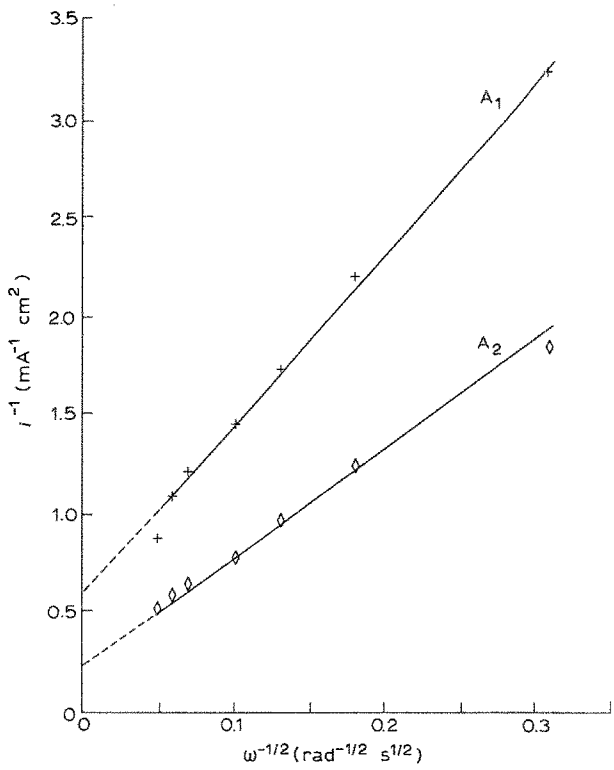

Fig. 7. Current peaks plotted as i_{A1}^{-1} and i_{A2}^{-1} against $\omega^{-1/2}$ for a tin disc electrode in 0.5 M $NaHCO_3$ solution, at $dE/dt = 2\,mV\,s^{-1}$.

scan no longer appeared and only one small cathodic peak C_1 occurred. As the positive potential limit was increased, the cathodic peak shifted to more negative potentials. The anodic charge greatly exceeded the cathodic charge for every potential limit. The films were slowly reduced prior to hydrogen evolution and some time (~ 10 min) was required at negative potential to clean the surface. The voltammogram obtained during the next cycle was easy to reproduce, which indicates that the electrode treatment was satisfactory. From this data it may be concluded that, at potentials more positive than -0.1 V, a strongly adherent film was formed on the electrode.

The voltammograms in Fig. 6 show the effect of the rotation speed ω from 0 to 3000 r.p.m. in the region of the two anodic peaks. As ω was increased, the height of the current peaks increased and the anodic charge and current were larger on the negative-going potential scan than on the preceding positive-going scan. The hysteresis of the anodic current and the shift of potential were found to be readily reproducible, independent of the number of potential cycles, and not due to the roughening of the electrode surface. However, when the anodic potential of the electrode exceeded -0.1 V, the hysteresis of the anodic current and the shift of the anodic potential disappeared.

The current of peaks A_1 and A_2 are presented in Fig. 7 as a graph of i^{-1} against $\omega^{-1/2}$. These relationships give straight lines and extrapolation of these plots to $\omega^{-1/2} \to 0$ yields values for dissolution currents free from diffusion according to the Levich theory [20]. These results suggest that the oxidation process was under mixed control of diffusion of ionic species into the solution and film formation reactions, the diffusion being dominant for low ω values.

Interestingly for $dE/dt > 50\,mV\,s^{-1}$ the hysteresis in the anodic current on the negative-going potential scan decreased and the reduction peak appeared. It is quite probable that the dissolved species do not have enough time to diffuse from the electrode and are therefore reduced. On the other hand, at $dE/dt = 1\,mV\,s^{-1}$, no potential shift was observed but the anodic current and charge on the negative-going potential scan were greater than in the forward direction. In this case, the product on the electrode had time to be dissolved and the bare tin surface and the dissolved species near the electrode are reoxidized.

In cyclic voltammograms, presented in Fig. 8, for a stationary electrode in 0.5 M $NaHCO_3$ solution at pH 8 and $10\,mV\,s^{-1}$, the reduction current was

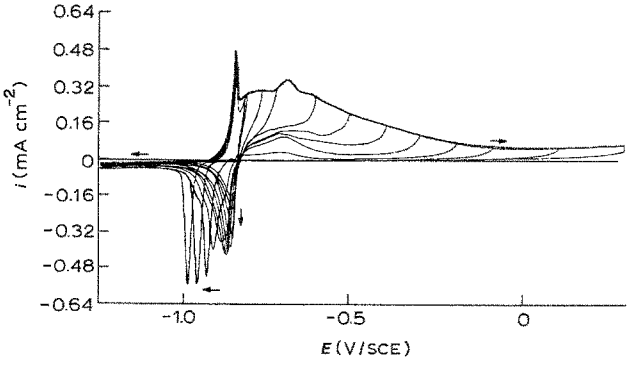

Fig. 8. Cyclic voltammograms reversed at progressively increasing positive-potential limits for a tin disc electrode in 0.5 M $NaHCO_3$ solution at pH 8, at $dE/dt = 10\,mV\,s^{-1}$.

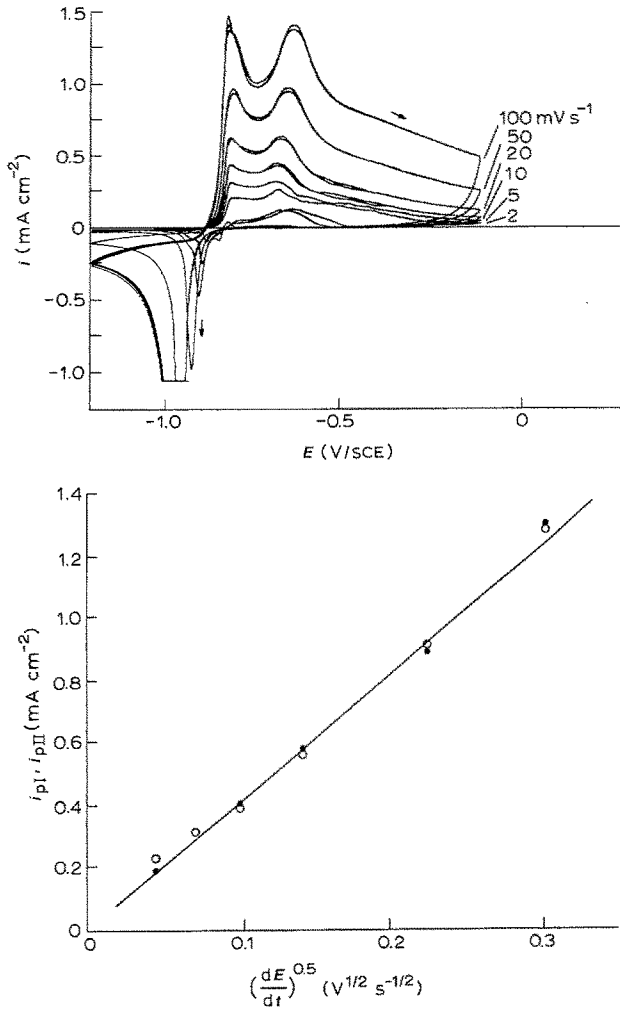

Fig. 9. (a) Cyclic voltammograms for a stationary tin disc electrode at sweep rates varying from 2 to 100 mV s^{-1} in 0.5 M $NaHCO_3$ solution at pH 8. (b) Current of peaks i_{A1} and i_{A2} against $(dE/dt)^{1/2}$.

observed for each potential scan limit. The influence of the sweep rate is shown in Fig. 9: the current of peaks i_{A1} and i_{A2} increased linearly with $(dE/dt)^{1/2}$ (Fig. 9b) with

$$\frac{i_{A1,A2}}{(dE/dt)^{1/2}} = 0.0041\ \mathrm{A\,cm^{-2}\,V^{-1/2}\,s^{1/2}} \qquad (5)$$

The potential of peak A_1 was independent of the sweep rate. However, as the scan rate was increased, the potential of peak A_2 moved slightly in the positive direction, which suggested that an irreversible process was involved at this peak.

The galvanostatic transient for the stationary tin electrode in 0.5 M $NaHCO_3$ with 100 μA cm^{-2} of the applied anodic current is presented in Fig. 10. Two potential plateaus at about −0.81 V and −0.72 V due to passivation of the electrode are followed by a fast increase of the potential up to oxygen evolution. The plateau potentials correlate well with the potentials of peaks A_1 and A_2 in the linear-sweep voltammograms.

4. Discussion

The anodic oxidation of tin (Fig. 1) can be divided into three potential regions: (i) a short active dissolution region; (ii) the dissolution-precipitation region and (iii) the large region of passivity electrode.

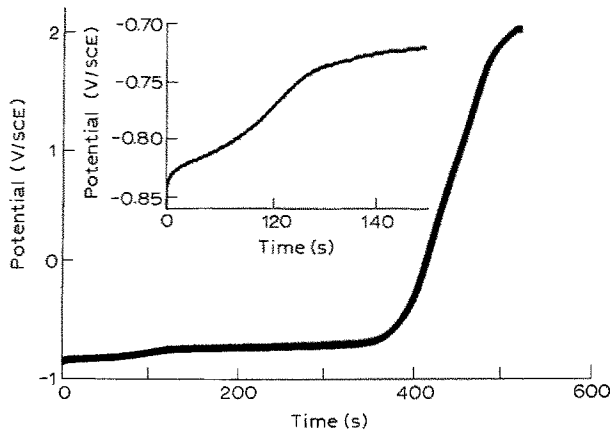

Fig. 10. Galvanostatic transient of potential against time for a stationary tin electrode in 0.5 M $NaHCO_3$ solution at pH 8, $i = 100\ \mu A\ cm^{-2}$.

4.1. *Active tin dissolution region*

The linear relationships of i against $\omega^{1/2}$ reported in Fig. 4 suggest that the diffusion of an ionic species into the solution is the r.d.s. of the dissolution process in this region of potential. The negative values of i at $\omega = 0$ may be attributed to a small hydrogen evolution contribution, since the applied potentials are 0.12 to 0.14 V lower than the reversible potential for the hydrogen evolution reaction at pH 8.

If the diffusing species are considered to be the anions already present in solution, i.e. OH^-, HCO_3^- and CO_3^{2-}, the theoretical relationships between i and $\omega^{1/2}$ may be calculated from Levich's equation [20]:

$$i = 0.62zFv^{-1/6}D_0^{2/3}[\mathrm{Co}]\omega^{1/2} \qquad (6)$$

where z is the charge of the diffusing species; v, the kinematic viscosity in $cm^2\ s^{-1}$; D_0 the diffuson coefficient of the diffusing species in $cm^2\ s^{-1}$; [Co] the concentration of the diffusing species in mol cm^{-3} and ω, the angular velocity of the electrode in rad s^{-1}. In the present case, v is $\sim 0.96 \times 10^{-2}\ cm^2\ s^{-1}$ [23] and D_0 is assumed to be $\sim 10^{-5}\ cm^2\ s^{-1}$ while $[OH^-] \sim 10^{-6}$ M, $[HCO_3^-] \sim 0.5$ M and $[CO_3^{2-}] \sim 2.3 \times 10^{-3}$ M (pKa = 10.33). The calculated i against $\omega^{1/2}$ relationships are illustrated in Fig. 4 for $[HCO_3^-]$ and $[CO_3^{2-}]$ species. Comparison of the calculated and experimental values clearly indicates that the diffusing species differ in nature from the ions already present in solution as OH^-, HCO_3^- and CO_3^{2-}.

The increase in the slope of i against $\omega^{1/2}$ with the applied potential suggests that the concentration of the diffusing species at the metal/solution interface also increases with the applied potential. The overall reaction for the generation of the diffusing species may be considered close to equilibrium, since the r.d.s. is the diffusion process. The reaction probably involves the transfer of two electrons, since $dE/d\log(di/d\omega^{1/2}) \sim 30$ mV dec^{-1}. The dissolution rate increased with the increase in $NaHCO_3$ concentration in solution, which suggests that HCO_3^-/CO_3^{2-} ions were

involved in the dissolution process, but no data about tin-carbonate complexes are available.

In alkaline solution without carbonate ions, the direct dissolution of tin as stannite or stannate is possible but these reactions are both thermodynamically and kinetically less probable [2] at pH 8. A mechanism involving the electrochemical formation of hydroxides or oxides followed by a chemical reaction to form the final product $HSnO_2^-$ is suggested instead. The stannite solutions are known to disproportionate into metallic tin and stannate [21].

4.2. *Dissolution-precipitation region*

The anodic current decay after peak A_1 (Fig. 1) may be explained by two processes: diffusion-controlled dissolution of tin and, subsequently, precipitation of porous oxides, hydroxides or hydroxycarbonate layers at the surface of the electrode. By correlating the peak potential, about -0.80 V, the semipassivation behaviour of tin in this region may be related to the following reactions [2, 13, 14, 16]:

$$\mathrm{Sn} + \mathrm{H_2O} = \mathrm{SnO} + 2\mathrm{H^+} + 2e^- \qquad E_{sce} = -0.82\,\mathrm{V} \qquad (7)$$

$$\mathrm{Sn} + 2\mathrm{OH^-} = \mathrm{Sn(OH)_2} + 2e^- \qquad E_{sce} = -0.808\,\mathrm{V} \qquad (8)$$

$$\mathrm{Sn} + 2\mathrm{H_2O} = \mathrm{SnO_2} + 4\mathrm{H^+} + 4e^- \qquad E_{sce} = -0.822\,\mathrm{V} \qquad (9)$$

$$\mathrm{SnO} + \mathrm{H_2O} = \mathrm{SnO_2} + 2\mathrm{H^+} + 2e^- \qquad E_{sce} = -0.824\,\mathrm{V} \qquad (10)$$

Equations 1 and 3 and the shape of the first peak (well defined and narrow) suggest that Sn(II) species are formed on the electrode surface.

As the electrode potential was increased, the current grew to reach a second maximum, peak A_2, at about -0.65 V. This behaviour can be represented by the following reactions [2, 13, 14, 16]:

$$\mathrm{Sn} + 4\mathrm{OH^-} = \mathrm{Sn(OH)_4} + 4e^- \qquad E_{sce} = -0.733\,\mathrm{V} \qquad (11)$$

$$\mathrm{Sn(OH)_2} + 2\mathrm{OH^-} = \mathrm{Sn(OH)_4} + 2e^- \qquad E_{sce} = -0.64\,\mathrm{V} \qquad (12)$$

$$\mathrm{SnO} + 2\mathrm{OH^-} + \mathrm{H_2O} = \mathrm{Sn(OH)_4} + 2e^- \qquad E_{sce} = -0.628\,\mathrm{V} \qquad (13)$$

The shift of the potential in the negative direction and the hysteresis of anodic current observed on the potentiodynamic curves between the sweeps in the positive-going and negative-going directions is attributed to the presence of HCO_3^-/CO_3^{2-} ions which causes the chemical dissolution of oxidation products at the electrode surface and the direct electro-oxidation process of tin at the bare electrode surface. Both these reactions explain the harmful effect of bicarbonate ions on tin, compared to other anions such as borate. The dissolution rate increased with the rotation speed and the $NaHCO_3$ concentration.

In the case of stationary electrode, the fact that the potential at peak A_1 was independent of the potential sweep rate suggests that the system is reversible, the concentration of species C_l^* in the bulk of the solution can be evaluated from the experimental value for $i_{A1}/(dE/dt)^{1/2} = 0.0041\,\mathrm{A\,cm^{-2}\,V^{-1/2}\,s^{1/2}}$ and the equation for the peak current in linear potential sweep voltammetry [22]

$$i_p = 2.69 \times 10^5 n^{3/2} A D^{1/2} (dE/dt)^{1/2} C_l^* \qquad (14)$$

at 25° C, for A in cm^2, $D_l \sim 10^{-5}\,cm^2\,s^{-1}$, dE/dt in $V\,s^{-1}$, C_l^* in $mol\,cm^{-3}$, i_p in A.

The calculations for $n = 2$ give $C_l^* = 1.2 \times 10^{-3}$ M and, for $n = 4$, $C_l = 0.3 \times 10^{-3}$ M. Taking into consideration the concentration of $[OH^-] \sim 10^{-6}$ M, $[HCO_3^-] \sim 0.5$ M and $[CO_3^{2-}] \sim 2.3 \times 10^{-3}$ M, (pKa = 10.33), it is deduced that the reaction is controlled by the diffusion of CO_3^{2-} ions from the bulk solution to the electrode surface.

4.3. *Electrode passivity*

In the region of positive potentials, a coherent, highly passivating film is formed at the electrode surface. The second peak, A_2, with a broad decreasing side, may reflect the chemical reactions to a more stable configuration. Most probably, a dehydration process occurs which involves multiple step reactions leading to the formation of SnO_2. Normally these reactions are very slow. The anodic current in this potential region was independent of the $NaHCO_3$ concentration in solution. In the negative potential sweep direction, the film was slowly reduced at potentials before hydrogen evolution occurs. The compact thin layer of SnO_2 is more likely responsible for the complete passivation of the electrode, since it is the most thermodynamically stable oxidation compound. However, the film composition cannot be determined electrochemically because the equilibrium potentials corresponding to the different possible reactions are very close. In this region of potential, oxidation is a solid-state process leading to the formation of the passivating film principally attributed to SnO_2.

Acknowledgements

Financial support from Hydro-Québec is gratefully acknowledged.

References

[1] S. N. Shah, D. E. Davies, *Electrochim. Acta* **8** (1963) 663.
[2] A. M. Shams El Din, F. M. Abd El Wahab, *ibid.* **9** (1964) 883.
[3] S. A. Awad, A. Kassab, *J. Electroanal. Chem.* **20** (1969) 203; **26** (1970) 127.
[4] B. N. Stirrup, N. A. Hampson, *ibid.* **67** (1976) 45, 57.
[5] T. Dickinson, S. Lotfi, *Electrochim. Acta* **23** (1978) 513, 995.
[6] H. Do Duc, P. Tissot, *J. Electroanal. Chem.* **102** (1979) 59.
[7] *Idem, Corrosion Sci.* **19** (1979) 179.
[8] V. S. Muralidharan, K. Thangavel, K. S. Rajagopalan, *Electrochim. Acta* **28** (1983) 703.

[9] R. O. Ansell, T. Dickinson, A. F. Povey, P. M. A. Sherwood, *J. Electrochem. Soc.* **124** (1977) 1360.
[10] T. D. Burleigh, H. Gerischer, *ibid.* **135** (1988) 2938.
[11] D. E. Davies, S. N. Shah, *Electrochim. Acta* **8** (1963) 703.
[12] S. D. Kapusta, N. Hackerman, *ibid.* **25** (1980) 1001, 1625.
[13] E. Deltombe, N. de Zoubov, M. Pourbaix, Rapport Tech. R. T. 25 du CEBELCOR (1955).
[14] M. Pourbaix, 'Atlas of Electrochemical Equilibria in Aqueous Solutions', 2nd ed., NACE Houston, USA (1974) p. 475.
[15] C. I. House, G. H. Kelsall, *Electrochim. Acta* **29** (1984) 1459.
[16] W. M. Latimer, 'Oxidation Potentials', 2nd ed., Prentice-Hall, New Jersey (1952).
[17] Z. Galus, in 'Encyclopedia of the Electrochemistry of the Elements' (edited by A. J. Bard), vol. 4, Dekker, New York (1975).
[18] 'Standard Potentials in Aqueous Solution' (edited by A. J. Bard, R. Parsons and J. Jordan), Dekker, New York (1985).
[19] R. Gilbert, Tech. Rapport IREQ – 4150b, Institut de Recherche d'Hydro-Québec, Varennes (Qué), April 1988.
[20] V. G. Levich, 'Physiochemical Hydrodynamics', Prentice-Hall, Englewood Cliffs, New York (1966).
[21] G. Charlot, 'L'Analyse quantitative et les réactions en solution', 4th ed., Masson, Paris (1957).
[22] A. J. Bard, L. R. Faulkner, 'Electrochemical Methods', John Wiley & Son, New York (1980).
[23] R. Parson, 'Handbook of Electrochemical Constants', Butterworths, London (1959).